

On the dynamics of interdecadal thermocline depth and sea surface temperature variability in the low to mid-latitude Pacific Ocean

Shayne McGregor and Neil J. Holbrook

Department of Physical Geography, Macquarie University, Sydney, New South Wales, Australia

Scott B. Power

Bureau of Meteorology Research Centre, Melbourne, Victoria, Australia

Received 10 August 2004; revised 18 October 2004; accepted 22 November 2004; published 16 December 2004.

[1] The role of upper ocean dynamics in generating interdecadal sea surface temperature (SST) variations is investigated with the help of the Australian Bureau of Meteorology Research Centre coupled general circulation model (CGCM) and a first baroclinic mode (“shallow-water”) ocean model (SWM). An empirical orthogonal function analysis is performed on the lowpass filtered SST and vertically averaged temperature in the upper 300 m anomaly data output from a 100-year CGCM simulation. The dominant mode SST spatial pattern and time variability is consistent with the Interdecadal Pacific Oscillation. The SWM is forced by wind stresses from the CGCM 100-year simulation to investigate the role of oceanic Rossby and Kelvin wave propagation on thermocline depth variations. The SWM produces variability similar to the CGCM interdecadal variability. We conclude that large scale wind forced upper ocean dynamics play a dominant role in generating interdecadal upper ocean temperature variations on decadal and longer timescales. *INDEX TERMS:* 4255 Oceanography: General: Numerical modeling; 4544 Oceanography: Physical: Internal and inertial waves; 4572 Oceanography: Physical: Upper ocean processes; 4247 Oceanography: General: Marine meteorology. **Citation:** McGregor, S., N. J. Holbrook, and S. B. Power (2004), On the dynamics of interdecadal thermocline depth and sea surface temperature variability in the low to mid-latitude Pacific Ocean, *Geophys. Res. Lett.*, 31, L24201, doi:10.1029/2004GL021241.

1. Introduction

[2] The dominant mode of Pacific Ocean interdecadal sea surface temperature (SST) variability has been identified in the recent literature as the Interdecadal Pacific Oscillation (IPO) [Power *et al.*, 1999; Folland *et al.*, 1999]. The identification of the IPO in SST determined from instrumental records prompted the investigation of other climatic data sources in order to establish its characteristics. For example, Pacific Ocean coral records have been used to illustrate the existence of interdecadal SST variations prior to the instrumental record [Linsley *et al.*, 2000]. Investigations of rainfall records have led to a better understanding of the connection between IPO SST variations and climate changes in many of the Pacific Ocean’s surrounding continents, such as changes in the rainfall rates of North America, Alaska and Australia [Trenberth and Hurrell,

1994; Power *et al.*, 1999]. Power *et al.* [1999] identified a statistical relationship between IPO phase and the impact that ENSO has on rainfall, surface temperature, river flow and crop yield in Australia during the twentieth century. These studies demonstrate that our understanding of the Pacific Ocean’s interdecadal variability has increased in recent years following research interest in the phenomenon [e.g., Latif and Barnett, 1994; Power *et al.*, 1999]. However, the physical mechanisms underpinning these interdecadal SST anomalies are still a matter of debate, and hence the IPO is a research topic of much contemporary interest.

[3] Many different hypotheses have been proposed to explain the IPO (for reviews, see Latif [1998] and Miller and Schneider [2000]), but in view of the recent literature, there are five dominant theories. (i) A one way stochastic forcing was first proposed by Hasselmann [1976] and later developed further by Frankignoul *et al.* [1997], but the application of this theory to the Pacific showed that coupling of the ocean to the atmosphere was needed to produce a realistic interdecadal SST variation [Neelin and Weng, 1999]. (ii) Latif and Barnett [1994] hypothesise that interdecadal SST variations are controlled by the strength of the gyre circulation in the Pacific Ocean and that gyre strength is modulated by ocean-atmosphere interactions. (iii) Gu and Philander [1997] propose an oceanic bridge linking the extratropical and the tropical Pacific Ocean. This bridge allows water parcels to be transported along lines of constant density from the extratropics to the tropics, where they upwell and alter Pacific Ocean SSTs. (iv) McPhaden and Zhang [2002] hypothesize that the rate of Pacific Ocean equatorial upwelling and hence equatorial SST is governed by a decadal varying meridional overturning circulation. Finally, (v) Galanti and Tziperman [2003] proposed a mechanism whereby amplified Rossby waves travel from the midlatitude eastern Pacific boundary towards the equator where they modulate the thermocline depth and cause SST variations in the tropical Pacific on interdecadal timescales.

[4] The present study seeks to understand the contribution of wind stress forced upper ocean dynamics on interdecadal upper ocean temperature variations as represented in the sophisticated coupled general circulation model (CGCM) of the Australian Bureau of Meteorology Research Centre (BMRC). Analysis of results from the BMRC CGCM simulation reveals an interdecadal SST variation consistent with the IPO. These results are further investigated with the help of an ocean “shallow-water” model (SWM). The (two-dimensional) linear first baroclinic-mode (shallow-

water) ocean model is used to help quantify the role of planetary scale wave propagation (Rossby and Kelvin waves) on interdecadal timescale vertical movements of the pycnocline, that might be expected to affect corresponding SST and upper ocean heat content variations.

2. Models and Simulations

[5] The coupled general circulation model analyzed here is called BCM2.2 (BMRC coupled atmosphere/ocean/sea-ice general circulation model, version 2.2). BCM2.2 is based on an earlier version called BCM2.0 described by *Power et al.* [1998]. It has an improved atmosphere general circulation model called the BMRC unified atmospheric model (BAM) which is run at a horizontal resolution of R21, with 17 vertical levels [*Colman et al.*, 2001]. The ocean component is a global version of the GFDL modular ocean model (MOM) [*Pacanowski et al.*, 1991; *Power et al.*, 1995]. MOM is configured to have increased resolution in the tropical Pacific by varying the meridional spacing from 0.5° within 7° latitude of the equator, from where it gradually increases to a maximum of 5.8° near the poles. This configuration improves the simulation of interannual variability, including the El Niño-Southern Oscillation phenomenon. Full details of the OGCM used in this study can be found in *Power et al.* [1995, 1998].

[6] BCM2.2 incorporates flux adjustments to net surface heat flux, net surface freshwater flux, and the penetrating short wave component of the heat flux. Monthly varying flux adjustment fields are used to ensure the veracity of the seasonal cycle. No flux adjustments are applied to surface stresses. BCM2.2 was integrated for 200 years and the last 100 years are analyzed here.

[7] BCM2.2 has been shown to exhibit significant inter-annual variability in the tropical Pacific, realistic atmosphere and ocean circulations, and evidence of both Rossby and Kelvin wave propagation along the thermocline [*Power et al.*, 1998]. For the present paper, monthly averages of the CGCM wind stress components in the east and north directions, SST, and the vertically-averaged upper ocean temperature (VAT) (upper 300 m) have been interpolated onto a global $1^\circ \times 1^\circ$ grid.

[8] The SWM developed by Neil Holbrook for the MATLAB environment is represented as a $1/2$ -layer model of the stratified ocean where ocean dynamics are described by the linear shallow-water equations [e.g., *Philander*, 1990, pp. 106–108]. The upper and lower ocean density layers are separated by an interface (*the pycnocline*) that approximates the thermocline. The reduced gravity, g' , reflects the density difference between the upper and lower layers. We used a typical value of $g' = 0.0294 \text{ m s}^{-2}$ [*Tomczak and Godfrey*, 1994, p.37]. The lower layer is assumed to be motionless and infinitely deep. We prescribe the mean depth of the upper well mixed active layer as $H = 300 \text{ m}$ [*Tomczak and Godfrey*, 1994, p.37]. The corresponding first baroclinic mode gravity wave speed $c_1 \approx 3 \text{ m s}^{-1}$, while the long Rossby wave speed $C_R(\text{ms}^{-1})$ is given by $C_R = \beta(c_1^2/f^2)$, where $f(\text{s}^{-1})$ is the Coriolis parameter and $\beta(\text{m}^{-1} \text{s}^{-1})$ is the derivative of f northwards. Thermodynamics are ignored in this dynamic-only formulation. Motion in the upper layer is driven by the applied wind stress (per unit density), and the associated

response of the ocean is displayed by the vertical displacement of the pycnocline, and the horizontal components of the flow velocity.

[9] The monthly-averaged wind stresses generated in the 100-year BCM2.2 simulation were used to force the SWM configured for the low-mid latitude Pacific Ocean ($41^\circ\text{S}–41^\circ\text{N}$, $120^\circ\text{E}–68^\circ\text{W}$). The smoothed monthly wind stresses were updated every 30 days. The three output fields (pycnocline depth and the two horizontal velocity components) were generated on a $1^\circ \times 1^\circ$ grid and archived as 30-day snapshots throughout the 100-year simulation.

3. Analysis Methods

[10] The IPO (signal) was defined as the 3rd Empirical Orthogonal Function (EOF) of the lowpass filtered *near-global* SST [*Power et al.*, 1999; *Folland et al.*, 1999]. For the present study we investigate the decadal variability in the century timescale simulations based on anomalies of (i) the pycnocline depth from the SWM, and (ii) SST and VAT from the CGCM, focusing only on the Pacific domain. The fields were filtered using a Butterworth filter with a 13-year cut-off. Note that the initial 10 years of the SWM output have been discarded as the model ocean was perturbed from rest (i.e., without ocean spinup) and it took about 10 years for the ocean to reach quasi-equilibrium in the subtropics. Hence, the first 10 years of the CGCM SSTs and VAT were also removed for purposes of comparison.

[11] We performed an EOF analysis on the correlation matrix of the 13-year lowpass filtered SST and VAT from the CGCM and the pycnocline depth variations from the SWM to determine the important interdecadal scale modes of variability. Note that the EOF analysis was performed on 2° averages of the output fields in order to reduce the computational memory required.

4. Results

[12] The first mode from the EOF analysis of the 13-year lowpass filtered CGCM SST (hereafter SSTE0F1) accounts for approximately 30% of the total filtered SST variance (Figure 1a). Comparison of the spatial pattern of SSTE0F1 with the IPO SST signature as seen in Figure 2 of *Power et al.* [1999] reveals several similarities. Firstly, positive weightings in the tropical Pacific SSTE0F1 cover a very similar area to the IPO, with both having their highest positive values in the equatorial region at approximately 120°W . Secondly, the positively weighted region at approximately 40°S , 120°W corresponds to a similar region of positive weighting in the IPO SST signature. Finally, areas of zero and negative weighting are evident in the subtropical (gyre) regions of SSTE0F1 which correspond to the negatively weighted areas apparent in the aforementioned IPO signature. However, the spatial extent of the prevalent negative weighting seen in the gyre regions of the IPO signature is not reproduced in SSTE0F1. We do not expect that this difference is of any real consequence to our results as observational records reveal that variations in tropical Pacific SST lead variations in North Pacific SST [*Trenberth and Hurrell*, 1994]. Thus, variations of the gyre SSTs may be primarily due to feedbacks of an initial tropical Pacific

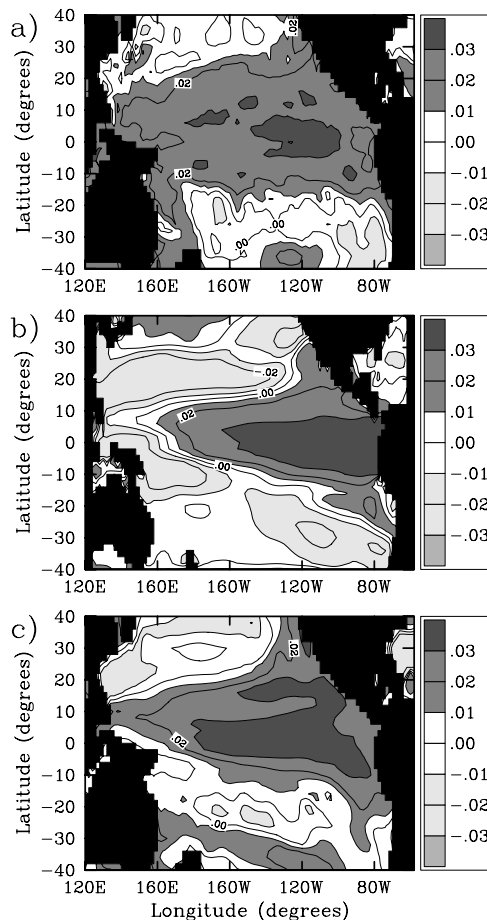


Figure 1. (a) The spatial pattern of SSTE OF1 which accounts for approximately 30% of the total filtered SST variance in BCM2.2; (b) The spatial pattern of PEOF1 which accounts for approximately 29% of the total filtered SWM pycnocline depth variance; (c) The spatial pattern of VATE OF1 which accounts for approximately 25% of the total filtered VAT variance in BCM2.2.

SST variation. Analysis of SSTE OF1s accompanying expansion coefficient time series (seen as the dotted line in Figure 2) reveals a slow decadal scale oscillation between positive and negative values. Taken together, the spatial pattern and time series of SSTE OF1 are consistent, at least in nature, with the observed IPO.

[13] The first EOF from the 13-year lowpass filtered pycnocline depth (hereafter PEOF1) from the SWM can be seen in Figure 1b. This mode accounts for approximately 29% of the total filtered pycnocline depth variance. Comparison of the spatial patterns of SSTE OF1 and PEOF1 (Figures 1a and 1b, respectively) reveals a broad similarity in the tropical Pacific region with both displaying positive weighting which narrows towards the western boundary. Despite this similarity in the tropical Pacific, there are several obvious differences outside this region. For example, either side of the positively weighted area of PEOF1, a band of negative weighting exists that extends diagonally from about 35° north and south of the equator at the east Pacific boundary to the western equatorial Pacific boundary which has no equivalent in SSTE OF1. These differences might be expected when considering the relationship be-

tween thermocline depth and SST in the tropical Pacific. For example, *Zelle et al.* [2004] demonstrate a direct correlation between thermocline depth and SST in the equatorial region east of 160°W . However, west of 160°W , no significant correlation is evident [*Zelle et al.*, 2004]. Hence, direct assessment of the SWM pycnocline depth variations against the BCM2.2 SST results across the *entire* Pacific basin can only be achieved by considering an alternatively derived BCM2.2 output field.

[14] A robust correlation between thermocline depth and upper ocean heat content in the tropical Pacific Ocean (to 15° latitude) is detailed by *Rebert et al.* [1985]. This relationship is utilized here to compare the average upper ocean temperature in BCM2.2 against the SWM results. BCM2.2 average upper ocean temperature (VAT) will be used as a proxy for upper ocean heat content in this comparison. The EOF analysis of the 13-year lowpass filtered VAT determined from BCM2.2 output produced a first mode (hereafter VATE OF1) that accounts for approximately 25% of the total filtered variance (Figure 1c). Comparison of the spatial pattern of VATE OF1 with PEOF1 again reveals an obvious similarity. Both have a large positively weighted area that meridionally covers the tropics from approximately 20°N/S at the eastern Pacific boundary narrowing to a minimum latitudinal extent at the western boundary. Also, either side of this positively weighted tropical Pacific pattern in both Figures 1b and 1c, bands of negative weighting also exist that extend diagonally from approximately 35° either side of the equator at the east Pacific boundary to the western equatorial Pacific boundary.

[15] Comparison of the corresponding expansion coefficients for SSTE OF1 and VATE OF1 (Figure 2, lines respectively in dotted and dashed) with PEOF1 (Figure 2, solid line) shows considerable similarity between the three time series. Both of the BCM2.2 fields and SWM pycnocline depth time variations display a positive correlation over the majority of the simulation period. The correlation coefficient between the time series of SSTE OF1 and PEOF1 is approximately 0.63 (significant at the 99% confidence level), while the correlation coefficient between the VATE OF1 and PEOF1 time series is 0.51 (significant at the 95% level). Both of these correlation coefficients are statistically significant based on the reduced effective number of degrees of freedom method outlined by *Davis* [1976].

5. Discussion

[16] In view of the five major existing theories proposed to explain the SST variations of the IPO, interesting and important features stand out on further investigation of the

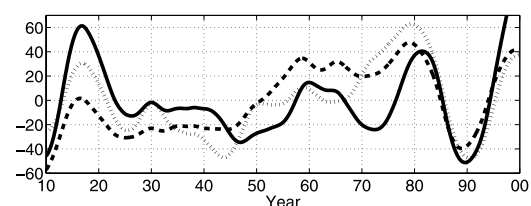


Figure 2. Expansion coefficients of SSTE OF1 (dotted), PEOF1 (solid) and VATE OF1 (dashed).

spatial pattern of our PEOF1. These are the negatively weighted bands that extend diagonally equatorward from the midlatitude eastern Pacific (near 35°) to the western equatorial boundary. These negative bands display a striking similarity when compared to the subduction paths proposed by *Gu and Philander* [1997] and the areas of baroclinic instability described by *Galanti and Tziperman* [2003]. Our analysis of an animation of the 13-year *filtered* SWM output reveals clear westward propagating signals in the regions defined by the bands of negative weighting at times when the expansion coefficient time series was at its maximum absolute value. The speed of these westward propagating anomalies was calculated to be approximately 5 cm/s (with the aid of a Hovmöller plot, not shown). These speeds are consistent with Rossby wave speeds produced in the SWM at 22°N. Hence, the negatively weighted bands either side of the equator in PEOF1 probably represent variability associated with westward propagating Rossby waves.

[17] A recent study by *Liu* [1999] displayed westward propagating Rossby waves that follow a similar trail as the aforementioned pathway linking the extratropics and Tropics. *Liu* [1999] shows that these “advective” type waves are normally generated by entrainment forcing, but they can also be generated through Ekman pumping of the thermocline. Considering our first baroclinic mode SWM is a dynamic-only model, with the upper layer having a prescribed constant density, the subduction of thermal anomalies along lines of constant density is not possible. Hence, the theory proposed by *Gu and Philander* [1997] cannot explain the interdecadal pycnocline depth variations seen in the SWM results. We conclude, therefore that Ekman pumping of the pycnocline is responsible for generating Rossby waves seen in the SWM output.

[18] *Galanti and Tziperman* [2003] explain that the arrival of Rossby waves at the equator can cause a low frequency modulation of the thermocline and hence interdecadal SST fluctuations, which is consistent with the positively weighted tropical Pacific region seen in PEOF1 (Figure 1b). Two additional SWM simulations (not shown here) were carried out to confirm that the equatorial pycnocline variability seen in PEOF1 was the result of ocean dynamic processes and not decadal SST generated variability in the overlying wind stress. These additional simulations were run in the absence of wind stress forcing from the equator to (a) $\pm 3^\circ$ and (b) $\pm 10^\circ$ latitude. Forcing outside of these regions was increased linearly over a further 5° latitude towards the BCM2.2 values. The equatorial pycnocline movements seen in PEOF1 were reproduced in both simulations despite the absence of wind stress in the equatorial zone, demonstrating that these pycnocline movements are an ocean dynamic response to off-equatorial wind stress variations.

[19] We conclude that Rossby waves generated as a result of Ekman pumping of the thermocline in the extratropics are responsible for the IPO-type pattern observed in the SWM simulations. Our results are consistent with the “planetary wave basin mode” theory proposed by *Galanti and Tziperman* [2003], leading us to believe that this theory

explains a significant proportion of the variability associated with the IPO.

References

- Colman, R. A., J. Fraser, and L. Rotstayn (2001), Climate feedbacks in a general circulation model incorporating prognostic clouds, *Clim. Dyn.*, *18*, 103–122.
- Davis, R. E. (1976), Predictability of sea surface temperature and sea level pressure anomalies over the North Pacific Ocean, *J. Phys. Oceanogr.*, *6*, 249–266.
- Folland, C. K., D. E. Parker, A. W. Colman, and R. Washington (1999), Large scale modes of ocean surface temperature since the late nineteenth century, in *Beyond El Niño: Decadal and Interdecadal Climate Variability*, edited by A. Navarra, pp. 73–102, Springer, New York.
- Frankignoul, C., P. Muller, and E. Zorita (1997), A simple model of the decadal response of the ocean to stochastic wind forcing, *J. Phys. Oceanogr.*, *27*, 1533–1546.
- Galanti, E., and E. Tziperman (2003), A midlatitudes-ENSO teleconnection mechanism via baroclinically unstable long Rossby waves, *J. Phys. Oceanogr.*, *33*, 1877–1888.
- Gu, D., and S. G. Philander (1997), Interdecadal climate fluctuations that depend on exchanges between the tropics and extratropics, *Science*, *275*, 805–807.
- Hasselmann, K. (1976), Stochastic climate models. Part I: Theory, *Tellus*, *28*, 473–485.
- Latif, M. (1998), Dynamics of interdecadal variability in coupled ocean-atmosphere models, *J. Clim.*, *11*, 602–624.
- Latif, M., and T. P. Barnett (1994), Causes of decadal climate variability over the North Pacific and North America, *Science*, *266*, 634–638.
- Linsley, B. K., G. M. Wellington, and D. P. Schrag (2000), Decadal sea surface temperature variability in the subtropical South Pacific from 1726 to 1997 A.D., *Science*, *290*, 1145–1148.
- Liu, Z. (1999), Forced planetary wave response in a thermocline gyre, *J. Phys. Oceanogr.*, *29*, 1036–1055.
- McPhaden, M. J., and D. Zhang (2002), Slowdown of the meridional overturning circulation in the upper Pacific Ocean, *Nature*, *415*, 603–608.
- Miller, A. J., and N. Schneider (2000), Interdecadal climate regime dynamics in the North Pacific Ocean: Theories, observations and ecosystem impacts, *Prog. Oceanogr.*, *47*, 355–379.
- Neelin, D. J., and W. Weng (1999), Analytical prototypes for ocean-atmosphere interaction at midlatitudes. Part I: Coupled feedbacks as a sea surface temperature dependent stochastic process, *J. Clim.*, *12*, 697–722.
- Pacanowski, R. C., K. Dixon, and A. Rosati (1991), The GFDL Modular Ocean model users guide, version 1.0, *Ocean Group Tech. Rep. 2*, 376 pp., Geophys. Fluid Dyn. Lab., Princeton Univ., Princeton, N. J.
- Philander, S. G. (1990), *El Niño, La Niña, and the Southern Oscillation*, 293 pp., Elsevier, New York.
- Power, S. B., R. Kleeman, F. Tseikin, and N. R. Smith (1995), A global version of the GFDL modular ocean model for ENSO studies, technical report, 18 pp., Bur. of Meteorol. Res. Cent., Melbourne, Victoria, Australia.
- Power, S. B., F. Tseikin, R. A. Coleman, and A. Sulaiman (1998), A coupled general circulation model for seasonal prediction and climate change research, *BMRC Res. Rep. 66*, 52 pp., Bur. of Meteorol. Res. Cent., Melbourne, Victoria, Australia.
- Power, S. B., T. Casey, C. Folland, A. Colman, and V. Mehta (1999), Interdecadal modulation of the impact of ENSO in Australia, *Clim. Dyn.*, *15*, 319–324.
- Rebert, J. P., J. R. Donguy, G. Eldin, and K. Wyrski (1985), Relations between sea level, thermocline depth, heat content and dynamic height in the tropical Pacific Ocean, *J. Geophys. Res.*, *90*, 11,719–11,725.
- Trenberth, K. E., and J. W. Hurrell (1994), Decadal atmosphere-ocean variations in the Pacific, *Clim. Dyn.*, *9*, 303–319.
- Tomczak, M., and S. J. Godfrey (1994), *Regional Oceanography: An Introduction*, 422 pp., Elsevier, New York.
- Zelle, H., G. Appeldoorn, G. Burgers, and G. J. V. Oldenborgh (2004), The relationship between sea surface temperature and thermocline depth in the tropical equatorial Pacific, *J. Phys. Oceanogr.*, *34*, 643–655.

N. J. Holbrook and S. McGregor, Department of Physical Geography, Macquarie University, Sydney, NSW 2109, Australia. (mcgregor@penman.es.mq.edu.au)

S. B. Power, Bureau of Meteorology Research Centre, Melbourne, Vic 3001, Australia.